

11-1 Computed Tomographic Reconstruction Based on X-ray Refraction Contrast

The X-ray refraction contrast technique was widely developed and applied in different fields of science which deal with nondestructive observation methods. As the name suggests, refraction contrast is the distribution of the X-ray intensity with respect to the deflection angle of the X-ray beam. This property of the contrast provides certain advantages over other properties such as absorption and phase-shift. The refraction contrast can show tiny details of the inner structure which are invisible using other types of X-ray imaging techniques. Another advantage of the X-ray refraction contrast method is for the observation of low-Z materials. The absorption coefficient of these materials may be two or three orders lower than the refraction index and therefore they may be almost invisible in absorption contrast. The refraction contrast however provides very beautiful images with very high contrast modulation. This property of the refraction contrast may be of great importance in medical X-ray applications. The advantages provided by the refraction contrast allow one to expect the same advantages for computed tomography (CT) reconstructions from the refraction contrast. Although there have been several attempts to realize this idea, they have either showed poor results or were even mathematically and physically incorrect. Therefore the main goal of this work was to make a full and correct model of the refraction-contrast-based CT reconstruction and then test it in an experiment. The problem included several semi-independent research directions: i) Theoretical consideration lead to the equation which served as the basis for the calculation:

$$i \Delta\alpha(\Theta, t) e^{i\phi} = \int_S |\nabla \tilde{n}(\mathbf{r})| e^{i\phi(t)} ds. \quad (1)$$

Here $\Delta\alpha$ is the deflection of the X-ray beam after penetration through the object. The integration is performed along the X-ray beam S which is described by the equation $t = x \cos \Theta + y \sin \Theta$, with Θ and t being the rotation position of the object and the distance of the beam from

the center of rotation. $\tilde{n}(\mathbf{r})$ has the relation to the refraction index field of $\tilde{n}(\mathbf{r}) = 1 - n(\mathbf{r})$. $\phi(\mathbf{r})$ is the angle between the X-ray beam and the gradient of the refraction index field $\nabla \tilde{n}(\mathbf{r})$. ii) Building the software for the reconstruction. Here it is necessary to note that the equations for the refraction-based CT-reconstruction are of a special form which does not allow one to adopt the well-developed absorption-based CT algorithms to our case. Therefore the method also requires new original software. The above CT equation also shows that the result of the reconstruction is not the refractivity itself, but its gradient. Therefore the gradient-to-field conversion is required for the method. We have developed and programmed an original algorithm for the gradient-to-field conversion. iii) The problem of the experimental derivation of the function $\Delta\alpha(\Theta, t)$ is not obvious and different techniques have been previously proposed. The most trust-worthy of these is the diffraction enhanced imaging (DEI) method presented in 1997. However the model used in DEI uses a Taylor expansion of the rocking curve and therefore is suitable only for limited ranges. The DEI method was slightly modified for the general case and used in our experiment. The modifications consider the actual rocking curve of the analyzing crystal instead of its Taylor approximation. iv) Experimental system for the data acquisition in accordance with the theory and the generalized DEI method. We have built a data acquisition system at BL-14B, as shown in Fig. 1. The system consists of collimating (M) and analyzing (A) crystals, a sample stage (O) with rotational (Θ) and translational (t) degrees of freedom, and a CCD camera as the detector. The results of the reconstruction of the experimentally acquired data reached all expectations. It was shown that the method is sensitive to very small structure elements which are invisible in other types of contrasts. We could successfully reconstruct the system of submicron cracks in a plastic sample (see Fig. 2(c)). Images in absorption and phase contrast of the same sample did not show any contrast corresponding to the cracks. The result of the reconstruction is shown in Fig. 2(b) as a 3D model and in Fig. 2(c) as an example of single slice reconstruction. A photograph of the sample is also shown for comparison (Fig. 2(a)). The

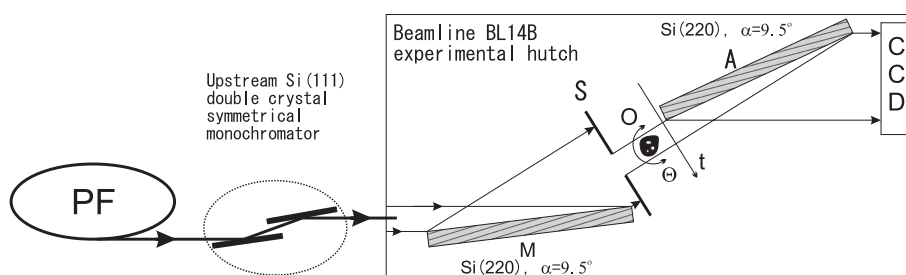


Figure 1
Experimental system.

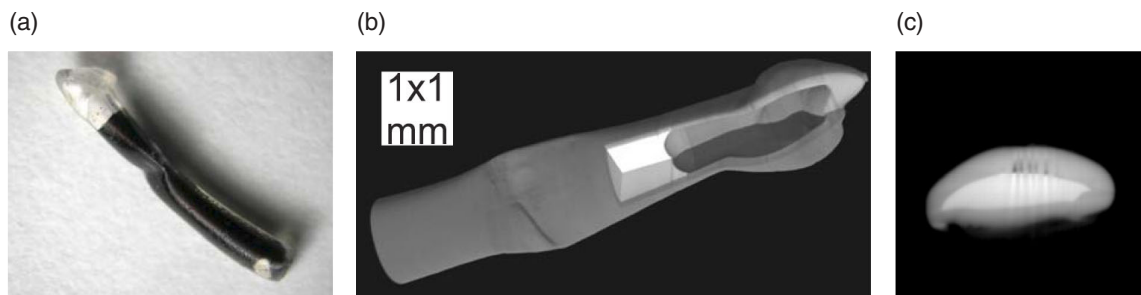


Figure 2
Results of the reconstruction. From left to write: (a) Photo of the object, (b) 3D representation of the reconstruction, (c) 2D reconstruction of one slice.

sample presented in these figures is a fragment of the refill for a ballpoint pen deformed with fire. The brighter contrast in Figs. 2(b) and 2(c) corresponds to the ink, while the gray contrast shows the plastic body of the refill.

A. Maksimenko¹, M. Ando^{1,2}, H. Sugiyama^{1,2}, and T. Yuasa³ (¹GUAS, ²KEK-PF, Yamagata Univ.,)

11-2 Development of Electron-ion Coincidence Spectroscopy and Electron Polar-angle-resolved Ion Coincidence Spectroscopy

When surface molecules are irradiated by soft X-rays, ion desorption may be stimulated by Auger processes (Auger-stimulated ion desorption, ASID, shown in Fig. 3). Experiments with coincident detection of photoelectrons and photoions (photoelectron photoion coincidence, PEPICO), as well as of Auger electrons and photoions (Auger electron photoion coincidence, AEPICO) are essential in order to elucidate the ASID mechanism, since using these techniques the ion yield and mass can be measured for selected photoemission and Auger processes. We have developed a new analyzer for electron-ion coincidence experiments, composed of a coaxially symmetric mirror electron energy analyzer (resolving power $E/\Delta E = 80\sim 120$; entrance solid angle 1.2 sr) and a miniature time-of-flight ion mass spectrometer (TOF-MS) (Fig. 4) [1, 2].

Furthermore, we have developed an electron polar-angle-resolved-ion coincidence apparatus consisting of a coaxially symmetric mirror electron energy analyzer and

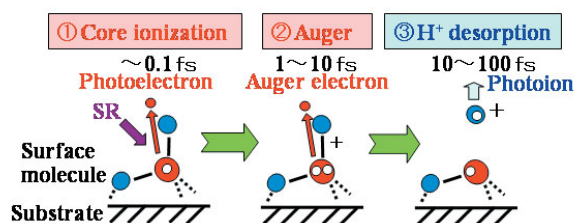


Figure 3
Auger stimulated ion desorption mechanism.

a miniature polar-angle-resolved TOF-MS. With this apparatus we can obtain information not only on the yield and mass but also on the kinetic energy and desorption polar angle of the coincidence ions. The TOF-MS consists of an electric field shield, an ion drift electrode with three meshes, and a microchannel plates detector assembly with three concentric anodes (Fig. 5). Using the SIMION 3D software we simulated ion trajectories for H^+ in the TOF-MS with a drift bias of -30 V. The results predicted the desorption angles of H^+ with a kinetic energy of 3 eV detected by the innermost anode, the intermediate anode, and the outermost anode to be $0^\circ \sim 17^\circ$, $22^\circ \sim 48^\circ$, and $57^\circ \sim 90^\circ$, respectively.

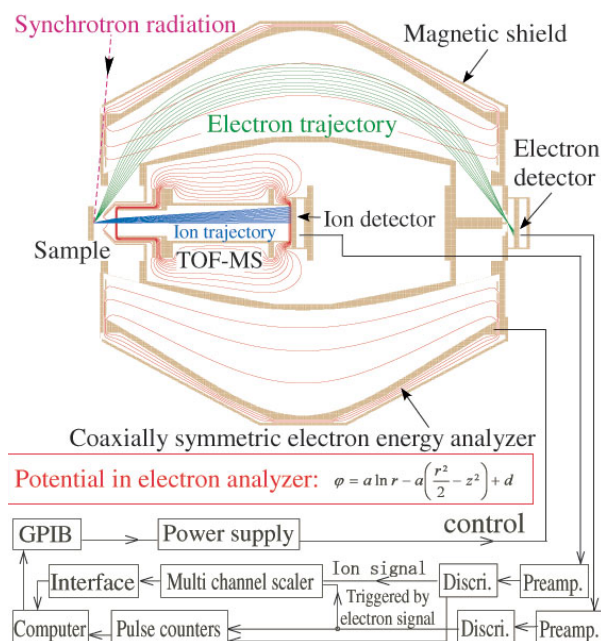


Figure 4
Electron ion coincidence analyzer.

Using these coincidence apparatuses, we have investigated the H^+ desorption induced by a resonant transition from the O 1s level to the $4a_1$ unoccupied orbital ($4a_1 \leftarrow O 1s$) of condensed water, and confirmed the following four-step ion desorption mechanism:-(1) $4a_1 \leftarrow O 1s$ transition, (2) extension of the HO-H distance in the $(O 1s)^1(4a_1)^1$ state within the lifetime of O 1s hole (ultrafast O-H extension), (3) spectator Auger transition leading to a state with two valence holes and an excited electron in the $4a_1$ orbital, and (4) H^+ desorption along the potential energy surface of the spectator Auger final state [3].

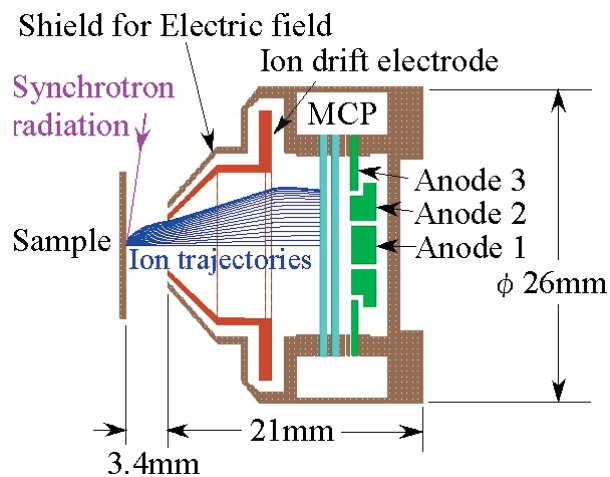


Figure 5
A miniature polar-angle-resolved TOF-MS.

We have been awarded the 29th Vacuum Society of Japan Award for Technical Development for our papers on these developments in electron ion coincidence spectroscopy [1, 4].

E. Kobayashi¹, K. Isari², K. Mase¹ (¹KEK-PF, ²Hiroshima Univ.)

References

- [1] K. Isari, H. Yoshida, T. Gejo, E. Kobayashi, K. Mase, S. Nagaoka and K. Tanaka, *J. Vac. Soc. Jpn.*, **46** (2003) 377 (in Japanese).
- [2] K. Isari, E. Kobayashi, K. Mase and K. Tanaka, *Surf. Sci.*, **528** (2003) 261.
- [3] A. Nambu, E. Kobayashi, M. Mori, K. K. Okudaira, N. Ueno and K. Mase, *Surface Science*, **593** (2005) 291, and references therein.
- [4] E. Kobayashi, K. Isari, M. Mori, K. Mase, K. Tanaka, K. Okudaira and N. Ueno, *J. Vac. Soc. Jpn.*, **47** (2004) 14 (in Japanese).